

---

# Learning Stable Classifiers by Transferring Unstable Features

---

**Yujia Bao**  
CSAIL MIT  
yujia@csail.mit.edu

**Shiyu Chang**  
MIT-IBM Watson AI Lab  
shiyu.chang@ibm.com

**Regina Barzilay**  
CSAIL MIT  
regina@csail.mit.edu

## Abstract

We study transfer learning in the presence of spurious correlations. We experimentally demonstrate that directly transferring the stable feature extractor learned on the source task may not eliminate these biases for the target task. However, we hypothesize that the unstable features in the source task and those in the target task are directly related. By explicitly informing the target classifier of the source task’s unstable features, we can regularize the biases in the target task. Specifically, we derive a representation that encodes the unstable features by contrasting different data environments in the source task. On the target task, we cluster data from this representation, and achieve robustness by minimizing the worst-case risk across all clusters. We evaluate our method on both text and image classifications. Empirical results demonstrate that our algorithm is able to maintain robustness on the target task, outperforming the best baseline by 22.9% in absolute accuracy across 12 transfer settings. Our code is available at <https://github.com/YujiaBao/Tofu>.

## 1 Introduction

In the context of transfer learning, regularizing spurious correlations is difficult due to data sparsity in the target task. While the source task may also exhibit spurious correlations, we can regularize the source model to be invariant against these unstable features using annotations from multiple data environments [2]. One would presume this is sufficient. Specifically, when we transfer the representation of this stable model, the spurious correlations are expected not to impact the target task as we have already regularized them in the source task. However, we empirically demonstrate that while the source classifier is not biased when making its final predictions, its internal representation can still encode unstable features. Figure 1 shows that in Colored MNIST, where the digit label is spuriously correlated with the image color [2], direct transfer by either re-using or fine-tuning the representation learned on the source task fails in the target task, performing no better than the majority baseline.

To address this challenge, we propose to inform the target classifier about unstable features. In general, we don’t know exactly which features are unstable, but often there is a direct connection between the spurious correlations in the target task and those in the source task. For instance, when classifying animals such as camels vs. cows, their background (desert vs. grass) may constitute a spurious correlation [6]. The same bias between the label and the background also persists in other related classification tasks (such as sheep vs. antelope). Therefore by transferring the knowledge of these unstable features, we can regularize their impact on the target task.

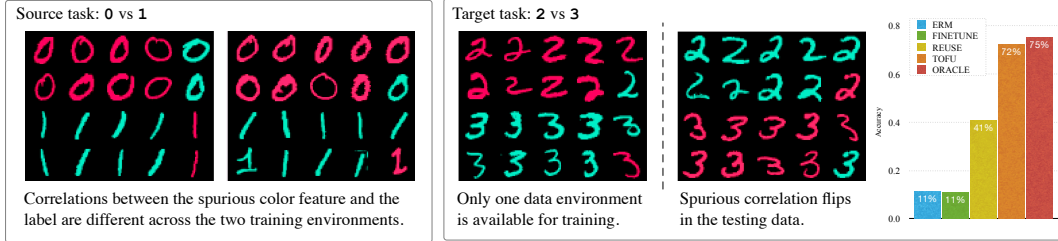


Figure 1: Transferring across tasks in Colored MNIST [2]. While we are able to learn a color-invariant model that achieves the performance of an oracle model (that has direct access to the unstable features) for the source task, directly transferring this model to the target task, by either reusing or fine-tuning its feature extractor, severely over-fits to the spurious correlation and underperforms the majority baseline (50%) on a test set where the spurious correlation flips. By explicitly transferring the unstable features, our algorithm TOFU (Transfer OF Unstable features) is able to reach the oracle performance.

Building on this idea, we first learn a representation that exposes the hidden unstable features in the source task. Following the work by Bao et al. [5], we use a classifier trained on one source environment to make predictions on another source environment. We prove that among examples with the same label value, those with the same prediction outcome have more similar unstable features than those with different predictions. Going back to our previous example, if the classifier uses the background to distinguish camels from cows, the camel images that are predicted correctly would have a desert background while those predicted incorrectly are likely to have a grass background. By encouraging examples with the same prediction result to stay close to each other, we derive a representation that encodes these hidden unstable features.

Given this unstable feature representation, we explicitly regularize the target classifier not to rely on the bias during training. Specifically, we cluster the target examples based on their unstable feature representation. Applying group distributionally robust optimization (DRO) [32] to minimize the worst-case risk over all clusters, we enforce the target classifier to be robust against different values of the unstable features. In the example above, animals would first be clustered based on different backgrounds, and the classifier should perform well regardless of the clusters (backgrounds).

We evaluate our approach, Transfer OF Unstable features (TOFU), on both image and text classification tasks. Our experiments first confirm our hypothesis that standard transfer approaches fail to learn a stable classifier for the target task. By explicitly transferring the unstable features, our method delivers significant performance gain (22.9% in absolute accuracy) over the best baseline across 12 transfer settings, and reaches the performance of an oracle model (with 0.3% difference) that has direct access to the unstable features. Qualitatively, we show that by contrasting different source environments, our method is able to encode examples based on the unstable features. Quantitatively, our generated clusters achieve 92% V-measure when evaluated against the ground truth unstable features.

## 2 Related work

**Removing bias by additional information:** Due to idiosyncrasies of the data collection process, annotations are often coupled with unwanted biases [8, 37, 28, 43]. To address this issue and learn robust models, researchers leverage extra information [7, 39, 17, 12, 15, 26]. One line of work assumes that the bias attributes are known and have been annotated for each example, e.g., group distributionally robust optimization (DRO) [18, 30, 33]. By defining groups based on these bias attributes, we explicitly specify the distribution family that we want to optimize over. However, identifying the hidden biases is time-consuming and often requires domain knowledge [44, 35]. To address this issue, another line of work [31, 22, 10, 19, 1, 2] only assumes access to a set of data environments. These environments are defined based on readily-available information of the data collection circumstances, such as location and time. The main assumption is that while spurious correlations vary across different environments, the association between the causal features and the label should stay the same. Thus, by learning a representation that is invariant across all environments, they alleviate the dependency on spurious features. In contrast to previous works, we don't have access to any additional information besides the labels in our target task. We show that we can achieve robustness by transferring the unstable features from a related source task.

**Removing bias by learning from mistakes** A number of recent approaches aim to draw connections between the model’s prediction mistakes and the bias. Sanh et al. [36], Utama et al. [40] find that weak models are more vulnerable to spurious correlations as they only learn shallow heuristics. By boosting from their mistakes, we can obtain a more robust model for some NLP tasks. In contrast, Sagawa et al. [34] points out that strong models actually over-fit unstable features more easily in image classification. From these contradictory results, it is unclear how the mistakes relate to the bias in general without any extra information. Most pertinent to our work, Bao et al. [5] presents an algorithm which uses a classifier trained on one data environment to make predictions on data from another environment. They show that the unstable correlation within the subset of incorrect predictions is opposite of that within the subset of correct predictions. They achieve robustness by minimizing the worst-case risk over these subsets. In this work, we advance this idea and draw a direct connection between the prediction results and the unstable features. We prove that the prediction results provide estimate the similarities of the examples in terms of their the unstable features. This enables us to learn a task-agnostic representation space that encodes the unstable features.

**Transferring robustness across tasks:** Prior work has also studied the transferability of adversarial robustness across tasks. For example, Hendrycks et al. [16], Shafahi et al. [38] show that by pre-training the model on a large-scale source task, we can improve the model robustness against adversarial perturbations over  $l_\infty$  norm. We note that these perturbations measure the smoothness of the classifier, rather than the stability of the classifier against spurious correlations. In fact, our results show that if we directly re-use or fine-tune the pre-trained feature extractor on the target task, the model will quickly over-fit to the unstable correlations present in the data. We propose to address this issue by explicitly inferring the unstable features using the source environments and use this information to guide the target classifier during training. Empirically, we demonstrate that our method is able to learn a robust classifier without multiple target environments.

### 3 Method

**Problem formulation** We consider the transfer problem from a source task to a target task. For the source task, we assume the standard setting [2] where the training data contain  $n$  environments  $E_1, \dots, E_n$ . Within each environment  $E_i$ , examples are drawn from the joint distribution  $P_i(x, y)$ . Following Woodward [42], we define unstable features  $\mathcal{Z}(x)$  as features that are *differentially* correlated with the label across the environments. We note that  $\mathcal{Z}(x)$  is unknown to the model.

For the target task, we assume that the label is *not* causally associated with the above unstable features  $\mathcal{Z}$ . However, due to collection biases, the target data may contain *spurious correlations* between the label and  $\mathcal{Z}$ . We don’t have multiple target environments to regularize this bias. Our goal is to transfer the knowledge that  $\mathcal{Z}$  is unstable in the source task, so that the target classifier will not rely on these spurious features.

**Overview** If the unstable features have been identified and annotated for the target task, we can simply apply group DRO to learn a stable classifier. By grouping examples based on the unstable features and minimizing the worst-case risk over these *manually-defined* groups, we can explicitly address the bias from these unstable features [18, 30, 33]. Coming back to our setup, we demonstrate that while these unstable features are not accessible, we can leverage the source environments to derive groups over the target data that are informative of these biases. Applying group DRO on these *automatically-derived* groups, we can eliminate the unstable correlations in the target task.

Our overall transfer paradigm is depicted in Figure 2. It consists of two parts: inferring unstable features from the source task (Section 3.1) and learning stable correlations for the target task (Section 3.2). In the first part, we operate on the source task and use a classifier trained on one environment to partition data from another environment based on the correctness of its predictions. Starting from the theoretical results in [5], we show that these partitions reflect the similarity of the examples in terms of their unstable features: among examples with the same label value, those that share the same prediction outcome have more similar unstable features than those with different predictions (Theorem 1). Based on this result, we can then derive a representation  $f_{\mathcal{Z}}$  where examples are distributed based on the unstable features  $\mathcal{Z}$ . In the second part, we cluster target examples into groups based on the learned unstable feature representation  $f_{\mathcal{Z}}$ . These *automatically-derived* groups correspond to different modes of the unstable features, and they act as approximations to the *manually-*

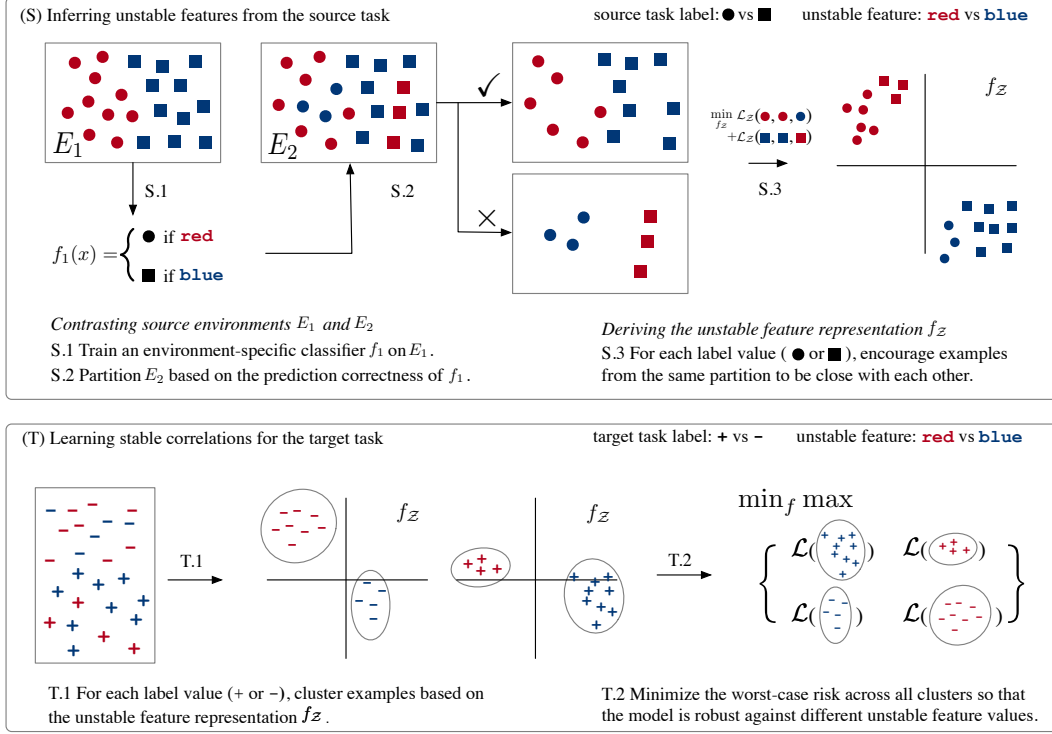


Figure 2: Our algorithm TOFU consists of two parts: inferring unstable features from the source task (Section 3.1) and learning stable correlations for the target task (Section 3.2). Note that we create partitions for all environment pairs. For ease of illustration, we only include using  $f_1$  to partition  $E_2$  in the figure. Best viewed in color.

defined groups in the oracle setting where unstable features are explicitly annotated. Finally, we use group DRO to obtain our robust target classifier by minimizing the worst-case risk over these groups.

**Extension to multiple source tasks:** Environments from a single source task may not describe all unwanted unstable features. In this situation, we would like to leverage multiple source tasks to compose their individual unstable features together. We can naturally extend TOFU to accomplish this goal by learning the unstable feature representation jointly across all source tasks. In this work, we focus on the basic setting and leave this extension to Appendix C.

### 3.1 Inferring unstable features from the source task

Given the data environments from the source task, we would like to 1) identify the unstable correlations across these environments; 2) learn a representation  $f_Z(x)$  that encodes the unstable features  $Z(x)$ . We achieve the first goal by contrasting the empirical distribution of different environments (Figure 2.S.1 and Figure 2.S.2) and the second goal by metric learning (Figure 2.S.3).

Let  $E_i$  and  $E_j$  be two different data environments. Bao et al. [5] shows that by training a classifier  $f_i$  on  $E_i$  and using it to make predictions on  $E_j$ , we can reveal the unstable correlations from its prediction results. Intuitively, if the unstable correlations are stronger in  $E_i$ , the classifier  $f_i$  will overuse these correlations and make mistakes on  $E_j$  when these stronger correlations do not hold.

In this work, we connect the prediction results directly to the unstable features. We show that the prediction results of the classifier  $f_i$  on  $E_j$  estimate the relative distance of the unstable features.

**Theorem 1** (Simplified). Consider examples in  $E_j$  with label value  $y$ . Let  $X_1^\vee, X_2^\vee$  denote two batches of examples that  $f_i$  predicted correctly, and let  $X_3^\times$  denote a batch of incorrect predictions. We use  $\bar{\cdot}$  to represent the mean across a given batch. Following the same assumption in [5], we have

$$\|\bar{Z}(X_1^\vee) - \bar{Z}(X_2^\vee)\|_2 < \|\bar{Z}(X_1^\vee) - \bar{Z}(X_3^\times)\|_2$$

almost surely for large enough batch size.<sup>1</sup>

The result makes intuitive sense as we would expect example pairs that share the same prediction outcome should be more similar than those with different prediction outcomes. We note that it is critical to look at examples with the same label value; otherwise, the unstable features will be coupled with the task-specific label in the prediction results.

While the value of the unstable features  $\mathcal{Z}(x)$  is still not directly accessible, Theorem 1 enables us to learn a feature representation  $f_{\mathcal{Z}}(x)$  that preserves the distance between the examples in terms of their unstable features. We adopt standard metric learning [11] to minimize the following triplet loss:

$$\mathcal{L}_{\mathcal{Z}}(X_1^{\checkmark}, X_2^{\checkmark}, X_3^{\times}) = \max(0, \|\overline{f_{\mathcal{Z}}}(X_1^{\checkmark}) - \overline{f_{\mathcal{Z}}}(X_2^{\checkmark})\|_2^2 - \|\overline{f_{\mathcal{Z}}}(X_1^{\checkmark}) - \overline{f_{\mathcal{Z}}}(X_3^{\times})\|_2^2 + \delta), \quad (1)$$

where  $\delta$  is a hyper-parameter. By minimizing Eq (1), we encourage examples that have similar unstable features to be close in the representation  $f_{\mathcal{Z}}$ . To summarize, inferring unstable features from the source task consists of three steps (Figure 2.S):

- S.1** For each source environment  $E_i$ , train an environment-specific classifier  $f_i$ .
- S.2** For each pair of environments  $E_i$  and  $E_j$ , use classifier  $f_i$  to partition  $E_j$  into two sets:  $E_j^{i\checkmark}$  and  $E_j^{i\times}$ , where  $E_j^{i\checkmark}$  contains examples that  $f_i$  predicted correctly and  $E_j^{i\times}$  contains those predicted incorrectly.
- S.3** Learn an unstable feature representation  $f_{\mathcal{Z}}$  by minimizing Eq (1) across all pairs of environments  $E_i, E_j$  and all possible label value  $y$ :

$$f_{\mathcal{Z}} = \arg \min \sum_{y, E_i \neq E_j} \mathbb{E}_{X_1^{\checkmark}, X_2^{\checkmark}, X_3^{\times}} [\mathcal{L}_{\mathcal{Z}}(X_1^{\checkmark}, X_2^{\checkmark}, X_3^{\times})],$$

where batches  $X_1^{\checkmark}, X_2^{\checkmark}$  are sampled uniformly from  $E_j^{i\checkmark}|_y$  and batch  $X_3^{\times}$  is sampled uniformly from  $E_j^{i\times}|_y$  ( $\cdot|_y$  denotes the subset of  $\cdot$  with label value  $y$ ).

### 3.2 Learning stable correlations for the target task

Given the unstable feature representation  $f_{\mathcal{Z}}$ , our goal is to learn a target classifier that focuses on the stable correlations rather than using unstable features. Inspired by group DRO [33] we minimize the worst-case risk across groups of examples that are representative of different unstable feature values. However, in contrast to DRO, these groups are constructed automatically based on the previously learned representation  $f_{\mathcal{Z}}$ .

For each target label value  $y$ , we use the representation  $f_{\mathcal{Z}}$  to cluster target examples with label  $y$  into different clusters (Figure 2.T.1). Since these clusters capture different modes of the unstable features, they are approximations of the typical manually-defined groups when annotations of the unstable features are available. By minimizing the worst-case risk across all clusters, we explicitly enforce the classifier to be robust against unstable correlations (Figure 2.T.2). We note that it is important to cluster within examples of the same label, as opposed to clustering the whole dataset. Otherwise, the cluster assignment may be correlated with the target label.

Concretely, learning stable correlations for the target task has two steps (Figure 2.T).

- T.1** For each label value  $y$ , apply K-means ( $l_2$  distance) to cluster examples with label  $y$  in the feature space  $f_{\mathcal{Z}}$ . We use  $C_1^y, \dots, C_{n_c}^y$  to denote the resulting cluster assignment, where  $n_c$  is a hyper-parameter.
- T.2** Train the target classifier  $f$  by minimizing the worst-case risk over all clusters:

$$f = \arg \min \max_{i,y} \mathcal{L}(C_i^y),$$

where  $\mathcal{L}(C_i^y)$  is the empirical risk on cluster  $C_i^y$ .

Table 1: Pearson correlation coefficient between the spurious feature  $\mathcal{Z}$  and the label  $Y$  for each task. The validation environment  $E^{\text{val}}$  follows the same distribution as  $E_1^{\text{train}}$ . We study the transfer problem between different task pairs. For the source task  $S$ , the model can access  $E_1^{\text{train}}(S)$ ,  $E_2^{\text{train}}(S)$  and  $E^{\text{val}}(S)$ . For the target task  $T$ , the model can access  $E_1^{\text{train}}(T)$  and  $E^{\text{val}}(T)$ .

$\rho(\mathcal{Z}, Y)$	MNIST		BEER REVIEW			ASK2ME		WATERBIRD	
	ODD	EVEN	LOOK	AROMA	PALATE	PENE.	INCI.	WATER	SEA.
$E_1^{\text{train}}$	0.87	0.87	0.60	0.60	0.60	0.31	0.44	0.36	0.39
$E_2^{\text{train}}$	0.75	0.75	0.80	0.80	0.80	0.52	0.66	0.63	0.64
$E^{\text{val}}$	0.87	0.87	0.60	0.60	0.60	0.31	0.44	0.36	0.39
$E^{\text{test}}$	-0.11	-0.11	-0.80	-0.80	-0.80	0.00	0.00	0.00	0.00

## 4 Experimental setup

### 4.1 Datasets and settings

We evaluate our approach on both image classification and text classification. We start with controlled experiments on MNIST [23] and BeerReview [27], where we inject spurious features into the input. We then consider a practical setting on ASK2ME [3] and Waterbird [32], where the spurious feature corresponds to an attribute of the input and is unknown to the model.

For each dataset, we consider multiple tasks and study the transfer between these tasks. Specifically, for each task, we split its data into four environments:  $E_1^{\text{train}}$ ,  $E_2^{\text{train}}$ ,  $E^{\text{val}}$ ,  $E^{\text{test}}$ , where spurious correlations vary across the two training environments  $E_1^{\text{train}}$ ,  $E_2^{\text{train}}$ . For the source task  $S$ , the model can access both of its training environments  $E_1^{\text{train}}(S)$ ,  $E_2^{\text{train}}(S)$ . For the target task  $T$ , the model only has access to one training environment  $E_1^{\text{train}}(T)$ . We note that the validation set  $E^{\text{val}}(T)$  plays an important role in early-stopping and hyper-parameter tuning, especially when the distribution of the data is different between training and testing [14]. In this work, since we don't have access to multiple training environments on the target task, we assume that the validation data  $E^{\text{val}}$  follows the same distribution as the training data  $E_1^{\text{train}}$ . Table 1 summarizes the level of the spurious correlations for different tasks. Additional statistics can be found in Appendix B.1.<sup>2</sup>

**MNIST** We extend Arjovsky et al. [2]'s approach for generating spurious correlations and define two *multi-class* classification tasks: EVEN (5-way classification among digits 0, 2, 4, 6, 8) and ODD (5-way classification among digits 1, 3, 5, 7, 9). For each image, we first map its numeric digit value  $y^{\text{digit}}$  into its class id within the task:  $y^{\text{causal}} = \lfloor y^{\text{digit}}/2 \rfloor$ . This class id serves as the causal feature for the given task. We then sample the observed label  $y$ , which equals to  $y^{\text{causal}}$  with probability 0.75 and a uniformly random other label value with the remaining probability. With this noisy label, we now sample the spurious color feature: the color value equals  $y$  with  $\eta$  probability and a uniformly other value with the remaining probability. We note that since there are five different digits for each task, we have five different colors. Finally, we color the image according to the generated color value. For the training environments, we set  $\eta$  to 0.8 in  $E_1^{\text{train}}$  and 0.9 in  $E_2^{\text{train}}$ . We set  $\eta = 0.1$  in the testing environment  $E^{\text{test}}$ .

**Beer review** We consider the transfer among three *binary* aspect-level sentiment classification tasks: LOOK, AROMA and PALATE [24]. For each review, we follow Bao et al. [5] and append a pseudo token (art\_pos or art\_neg) based on the the sentiment of the given aspect (pos or neg). The probability that this pseudo token agrees with the sentiment label is 0.8 in  $E_1^{\text{train}}$  and 0.9 in  $E_2^{\text{train}}$ . In the testing environment, this probability reduces to 0.1. Unlike MNIST, there is no label noise added to the data.

**ASK2ME** ASK2ME [3] is a text classification dataset where the inputs are paper abstracts from PubMed. We study the transfer between two *binary* classification tasks: PENETRANCE (identifying whether the abstract is informative about the risk of cancer for gene mutation carriers) and INCIDENCE

<sup>1</sup>See Appendix A for the full theorem and proof.

<sup>2</sup>All data splits are available in the supplementary materials.

(identifying whether the abstract is informative about proportion of gene mutation carriers in the general population). By definition, both tasks are causally-independent of the diseases that have been studied in the abstract. However, due to the bias in the data collection process, Deng et al. [13] found that the performance varies (by 12%) when we evaluate based on different cancers. To assess whether we can remove such bias, we define two training environments for each task, where the correlations between the task label and the `breast_cancer` attribute (indicating the presence of breast cancer in the abstract) are different. Note that the model doesn't have access to the `breast_cancer` attribute during training. Following Sagawa et al. [32], we evaluate the performance on a balanced test environment where there is no spurious correlation between `breast_cancer` and the task label. This helps us understand the overall generalization performance across different input distributions.

**Waterbird** Waterbird is an image classification dataset where each image is labeled based on its bird class [41] and the background attribute (`water` vs. `land`). Following Sagawa et al. [32], we group different bird classes together and consider two *binary* classification tasks: SEABIRD (classifying 36 seabirds against 36 landbirds) and WATERFOWL (classifying 9 waterfowl against 9 *different* landbirds). This dataset is biased: seabirds and waterfowl mostly appear with a water background and landbirds mostly appear in the land. Similar to ASK2ME, we define two training environments for each task, where the correlations between the task label and the `background` attribute are different. At test time, we measure the generalization performance on a balanced test environment.

## 4.2 Baselines

We compare our algorithm against the following baselines:

ERM: We learn a classifier on the target task from scratch by minimizing the average loss across all examples. Note that this classifier is independent of the source task. Its performance reflects the deviation between the training distribution and the testing distribution of the target task.

REUSE: We first learn a stable model on the source task by contrasting different source environments [5]. We then directly transfer its feature extractor to the target task. By keeping this feature extractor fixed when learning the target classifier (a linear layer followed by Softmax activation), we hope the resulting model will not rely on these unstable features.

FINETUNE: Similar to REUSE except that we also update the feature extractor when training the target classifier. [38] has shown that FINETUNE can improve adversarial robustness of the target task.

MULTITASK: We adopt the standard multi-task learning approach [9] where the source model and the target model share the same feature extractor and are jointly trained together. For the source task, we first partition the source data into subsets with opposite spurious correlations [5]. During multi-task training, we minimize the worst-case risk over all these subsets for the source task and minimize the average empirical risk for the target task. MULTITASK is more flexible than REUSE since we can tune the feature extractor to fit the target data. Compared to FINETUNE, MULTITASK is more constrained as the source model will prevent over-utilizing unstable features during the joint training process.

ORACLE: We can use the hidden unstable features to define groups and train an oracle model using group DRO. For example, in task SEABIRD, this oracle model will minimize the worst-case risk over the following four groups: {seabird with water}, {seabird with land}, {landbird with water}, {landbird with land}. Like ERM, this oracle model is independent of the source task. It helps us analyze the robustness of our proposed algorithm separately from the inherent limitations (such as model capacity and data size) of the target task.

For fair comparison, all methods share the *same* representation backbone and the *same* hyperparameter search space. Implementation details can be found in Appendix B.2.

## 5 Results

Table 2 summarizes the results on four datasets. We observe that standard transfer methods (REUSE, FINETUNE, MULTITASK) fail to improve over the ERM baseline. On the other hand, TOFU consistently achieves the best performance across 12 transfer settings, outperforming the best baseline by 22.9% in absolute accuracy. While TOFU doesn't have access to the unstable features, by inferring them from the source environments, it matches the oracle performance with only 0.30% absolute difference.

Table 2: Target task accuracy of different methods on image classification (MNIST and WATERBIRD) and text classification (BEER REVIEW and ASK2ME). All methods are tuned based on a held-out validation set that follows from the same distribution as the target training data. Bottom right: standard deviation across 5 runs. Upper right: source task testing performance (if applicable).

	SOURCE	TARGET	ERM	REUSE	FINETUNE	MULTITASK	TOFU	ORACLE
MNIST	ODD	EVEN	12.3 $\pm$ 0.6	14.4 <sup>(70.9)</sup> <sub><math>\pm</math>1.0</sub>	11.2 <sup>(70.1)</sup> <sub><math>\pm</math>2.1</sub>	11.6 <sup>(69.6)</sup> <sub><math>\pm</math>0.6</sub>	<b>69.1</b> $\pm$ 1.6	68.7 $\pm$ 0.9
	EVEN	ODD	9.7 $\pm$ 0.6	19.2 <sup>(71.1)</sup> <sub><math>\pm</math>2.3</sub>	11.5 <sup>(71.1)</sup> <sub><math>\pm</math>1.2</sub>	10.1 <sup>(70.0)</sup> <sub><math>\pm</math>0.7</sub>	<b>66.8</b> $\pm$ 0.8	67.8 $\pm$ 0.5
BEER REVIEW	LOOK	AROMA	55.5 $\pm$ 1.7	31.9 <sup>(70.1)</sup> <sub><math>\pm</math>1.0</sub>	53.7 <sup>(70.1)</sup> <sub><math>\pm</math>1.4</sub>	54.1 <sup>(76.0)</sup> <sub><math>\pm</math>2.2</sub>	<b>75.9</b> $\pm$ 1.4	77.3 $\pm$ 1.3
	LOOK	PALATE	46.9 $\pm$ 0.3	22.8 <sup>(70.0)</sup> <sub><math>\pm</math>1.9</sub>	49.3 <sup>(73.2)</sup> <sub><math>\pm</math>2.1</sub>	52.8 <sup>(73.3)</sup> <sub><math>\pm</math>2.9</sub>	<b>73.8</b> $\pm$ 0.7	74.0 $\pm$ 1.2
	AROMA	LOOK	63.9 $\pm$ 0.6	40.1 <sup>(68.6)</sup> <sub><math>\pm</math>3.1</sub>	65.2 <sup>(66.4)</sup> <sub><math>\pm</math>1.8</sub>	64.0 <sup>(71.5)</sup> <sub><math>\pm</math>0.6</sub>	<b>80.9</b> $\pm$ 0.5	80.1 $\pm$ 0.6
	AROMA	PALATE	46.9 $\pm$ 0.3	14.0 <sup>(68.3)</sup> <sub><math>\pm</math>2.4</sub>	47.9 <sup>(63.2)</sup> <sub><math>\pm</math>3.3</sub>	50.0 <sup>(71.2)</sup> <sub><math>\pm</math>1.4</sub>	<b>73.5</b> $\pm$ 1.1	74.0 $\pm$ 1.2
	PALATE	LOOK	63.9 $\pm$ 0.6	40.4 <sup>(57.2)</sup> <sub><math>\pm</math>2.8</sub>	64.3 <sup>(60.1)</sup> <sub><math>\pm</math>2.7</sub>	63.1 <sup>(75.9)</sup> <sub><math>\pm</math>1.0</sub>	<b>81.0</b> $\pm$ 1.0	80.1 $\pm$ 0.6
	PALATE	AROMA	55.5 $\pm$ 1.7	23.1 <sup>(59.2)</sup> <sub><math>\pm</math>3.3</sub>	54.5 <sup>(58.7)</sup> <sub><math>\pm</math>1.2</sub>	56.5 <sup>(73.3)</sup> <sub><math>\pm</math>1.3</sub>	<b>76.9</b> $\pm$ 1.5	77.3 $\pm$ 1.3
ASK.	PENE	INCI.	79.3 $\pm$ 1.3	71.7 <sup>(72.7)</sup> <sub><math>\pm</math>0.5</sub>	79.3 <sup>(71.2)</sup> <sub><math>\pm</math>0.8</sub>	71.1 <sup>(73.5)</sup> <sub><math>\pm</math>1.4</sub>	<b>83.2</b> $\pm$ 1.8	84.8 $\pm$ 1.2
	INCI.	PENE.	71.6 $\pm$ 1.8	64.1 <sup>(83.4)</sup> <sub><math>\pm</math>1.5</sub>	72.0 <sup>(83.4)</sup> <sub><math>\pm</math>3.1</sub>	61.9 <sup>(82.4)</sup> <sub><math>\pm</math>0.7</sub>	<b>78.1</b> $\pm$ 1.4	78.3 $\pm$ 0.9
BIRD	WATER	SEA.	81.8 $\pm$ 4.3	87.8 <sup>(99.5)</sup> <sub><math>\pm</math>1.1</sub>	82.0 <sup>(99.5)</sup> <sub><math>\pm</math>4.0</sub>	88.0 <sup>(99.5)</sup> <sub><math>\pm</math>0.9</sub>	<b>93.1</b> $\pm$ 0.4	93.7 $\pm$ 0.7
	SEA.	WATER	75.1 $\pm$ 6.3	94.6 <sup>(93.3)</sup> <sub><math>\pm</math>1.6</sub>	78.2 <sup>(93.1)</sup> <sub><math>\pm</math>8.1</sub>	93.5 <sup>(92.7)</sup> <sub><math>\pm</math>1.9</sub>	<b>99.0</b> $\pm$ 0.4	98.9 $\pm$ 0.5
Average			55.2	43.7	55.8	56.4	79.3	79.6

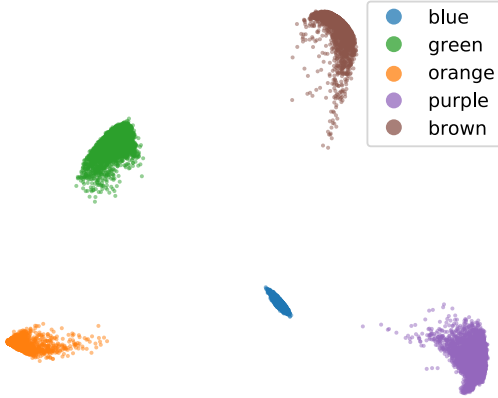


Figure 3: PCA visualization of the unstable feature representation  $f_Z$  for examples in MNIST EVEN.  $f_Z$  is trained on MNIST ODD. While the spurious color features are not accessible, TOFU is able to identify them by contrasting different source environments.

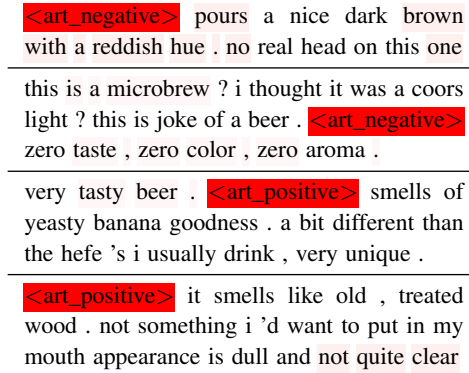


Figure 4: Word importance for the unstable feature representation  $f_Z$  trained on BEER LOOK. We observe that  $f_Z$  behaves as a spurious token detector: it focuses mostly on the spurious token despite the presence of sentiment words.

**Why do the baselines behave so differently across different datasets?** As [4] pointed out, the transferability of the low-level features is very different in image classification and in text classification. For example, the keywords for identifying the sentiment of LOOK are very different from the ones for PALATE. Thus, fine-tuning the feature extractor is crucial. This explains why REUSE underperforms other baselines on text data. Conversely, in image classification, the low-level patterns (such as edges) are more transferable across tasks. Directly reusing the feature extractor helps improve model stability against spurious correlations. Finally, we note that since TOFU transfers the unstable features instead of the task-specific causal features, it performs robustly across all the settings.

Table 3: Quantitative evaluation of the generated clusters against the ground truth unstable features. The ERM baseline clusters target example based on a feature extractor learned on the source task. For both methods, we generate two clusters for each target label value and report the average performance across all label values. We observe that the ERM representation, while biased by the spurious correlations, fails to recover the ground truth unstable features. By explicitly contrasting the source environments, TOFU derives clusters that are highly-informative of the unstable features.

	SOURCE	TARGET	Homogeneity		Completeness		V measure	
			ERM	TOFU	ERM	TOFU	ERM	TOFU
MNIST	ODD	EVEN	0.2584	<b>0.6820</b>	0.2714	<b>0.9561</b>	0.2535	<b>0.7960</b>
	EVEN	ODD	0.1454	<b>0.6764</b>	0.0983	<b>0.9988</b>	0.1173	<b>0.8055</b>
BEER REVIEW	LOOK	AROMA	0.0019	<b>0.9256</b>	0.0014	<b>0.9218</b>	0.0016	<b>0.9236</b>
	LOOK	PALATE	0.0088	<b>0.9095</b>	0.0064	<b>0.8988</b>	0.0074	<b>0.9039</b>
	AROMA	LOOK	0.0017	<b>1.0000</b>	0.0012	<b>1.0000</b>	0.0014	<b>1.0000</b>
	AROMA	PALATE	0.0088	<b>1.0000</b>	0.0064	<b>1.0000</b>	0.0074	<b>1.0000</b>
	PALATE	LOOK	0.0005	<b>0.9816</b>	0.0003	<b>0.9811</b>	0.0004	<b>0.9813</b>
	PALATE	AROMA	0.0028	<b>0.9585</b>	0.0020	<b>0.9561</b>	0.0024	<b>0.9573</b>

*Is TOFU able to identify the unstable features?* Yes. For image classification, we visualize the unstable feature representation produced by  $f_Z$  on MNIST EVEN. Figure 3 demonstrates that while  $f_Z$  only sees source examples (ODD) during training, it is able to distribute target examples based on their unstable color features. For text classification, we visualize the word importance of  $f_Z$  on BEER LOOK. Figure 4 shows that  $f_Z$  primarily focuses on the spurious token when generating the representation.

*How many clusters to generate?* We study the effect of the number of clusters on ASK2ME. Figure 5 shows that while generating more clusters in the unstable feature space  $f_Z$  reduces the variance, it doesn’t improve the performance by much. This is not very surprising as the training data is primarily biased by a single `breast_cancer` attribute. We expect that having more clusters will be beneficial for tasks with more sophisticated underlying biases.

*How do the generated clusters compare to the oracle groups?* We quantitatively evaluate the generated clusters based on three metrics: *homogeneity* (whether each cluster contain only examples with the same unstable feature value), *completeness* (whether examples with the same unstable feature value belong to the same cluster), and *V-measure* (the harmonic mean of homogeneity and completeness). From Table 3, we see that TOFU is able to derive clusters that resemble the oracle groups on BEER REVIEW.

In MNIST, we note that since we generate two clusters for each label value and there are five different colors, it is impossible to recover the oracle groups. However, TOFU still achieves almost perfect completeness. For comparison, we directly apply K-means clustering to the feature representation learned by ERM on the source environments. Although this representation is biased by the unstable feature, the resulting clusters fail to uncover the oracle groups.

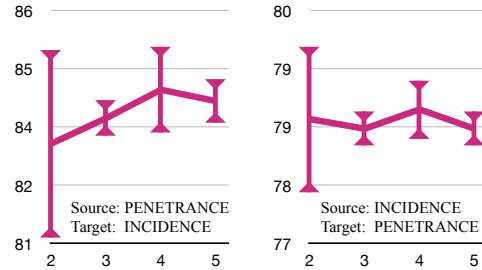


Figure 5: Accuracy of TOFU on ASK2ME as we vary the number of clusters  $n_c$  generated for each label value. Empirically, we see that while having more clusters doesn’t improve the performance, it helps reduce the variance.

## 6 Conclusion and social impacts

We study transfer learning in the presence of spurious correlations. Current transfer techniques fail as the target model is not aware of these spurious correlations during training. In this paper, we propose to explicitly inform the target model about the unstable features, therefore enabling it to regularize the impact of the biases. Specifically, our algorithm learns an unstable feature space by

contrasting different source environments. On the target task, we cluster examples using this unstable feature space. By minimizing the worst-case risk over all clusters, we explicitly enforce the target classifier to be robust against different values of the unstable feature. Experimental results validate that our algorithm is able to generate clusters that are informative of the unstable feature and learn a stable classifier. We do not recognize any potential negative social impacts of our work. Instead, by eliminating biases from the model, our algorithm promotes the fairness of AI.

## Acknowledgments and Disclosure of Funding

This paper is dedicated to the memory of our beloved family member Tofu, who filled our lives with so many wuffs and wuvs.

We thank the MIT NLP group for their thoughtful feedback. Research was sponsored by the United States Air Force Research Laboratory and the United States Air Force Artificial Intelligence Accelerator and was accomplished under Cooperative Agreement Number FA8750-19-2-1000. The views and conclusions contained in this document are those of the authors and should not be interpreted as representing the official policies, either expressed or implied, of the United States Air Force or the U.S. Government. The U.S. Government is authorized to reproduce and distribute reprints for Government purposes notwithstanding any copyright notation herein.

## References

- [1] K. Ahuja, K. Shanmugam, K. Varshney, and A. Dhurandhar. Invariant risk minimization games. In *International Conference on Machine Learning*, pages 145–155. PMLR, 2020.
- [2] M. Arjovsky, L. Bottou, I. Gulrajani, and D. Lopez-Paz. Invariant risk minimization. *arXiv preprint arXiv:1907.02893*, 2019.
- [3] Y. Bao, Z. Deng, Y. Wang, H. Kim, V. D. Armengol, F. Acevedo, N. Ouadaoui, C. Wang, G. Parmigiani, R. Barzilay, D. Braun, and K. S. Hughes. Using machine learning and natural language processing to review and classify the medical literature on cancer susceptibility genes. *JCO Clinical Cancer Informatics*, (3):1–9, 2019. doi: 10.1200/CCI.19.00042. URL <https://doi.org/10.1200/CCI.19.00042>. PMID: 31545655.
- [4] Y. Bao, M. Wu, S. Chang, and R. Barzilay. Few-shot text classification with distributional signatures. In *International Conference on Learning Representations*, 2019.
- [5] Y. Bao, S. Chang, and R. Barzilay. Predict then interpolate: A simple algorithm to learn stable classifiers. In *International Conference on Machine Learning (ICML)*, 2021.
- [6] S. Beery, G. Van Horn, and P. Perona. Recognition in terra incognita. In *Proceedings of the European Conference on Computer Vision (ECCV)*, pages 456–473, 2018.
- [7] Y. Belinkov, A. Poliakov, S. M. Shieber, B. Van Durme, and A. M. Rush. Don’t take the premise for granted: Mitigating artifacts in natural language inference. In *Proceedings of the 57th Annual Meeting of the Association for Computational Linguistics*, pages 877–891, 2019.
- [8] J. Buolamwini and T. Gebru. Gender shades: Intersectional accuracy disparities in commercial gender classification. In *Conference on fairness, accountability and transparency*, pages 77–91, 2018.
- [9] R. Caruana. Multitask learning. *Machine learning*, 28(1):41–75, 1997.
- [10] S. Chang, Y. Zhang, M. Yu, and T. S. Jaakkola. Invariant rationalization. *arXiv preprint arXiv:2003.09772*, 2020.
- [11] G. Chechik, V. Sharma, U. Shalit, and S. Bengio. Large scale online learning of image similarity through ranking. 2010.
- [12] C. Clark, M. Yatskar, and L. Zettlemoyer. Don’t take the easy way out: Ensemble based methods for avoiding known dataset biases. In *Proceedings of the 2019 Conference on Empirical Methods in Natural Language Processing and the 9th International Joint Conference on Natural Language Processing (EMNLP-IJCNLP)*, pages 4060–4073, 2019.

- [13] Z. Deng, K. Yin, Y. Bao, V. D. Armengol, C. Wang, A. Tiwari, R. Barzilay, G. Parmigiani, D. Braun, and K. S. Hughes. Validation of a semiautomated natural language processing-based procedure for meta-analysis of cancer susceptibility gene penetrance. *JCO clinical cancer informatics*, 3:1–9, 2019.
- [14] I. Gulrajani and D. Lopez-Paz. In search of lost domain generalization. *arXiv preprint arXiv:2007.01434*, 2020.
- [15] H. He, S. Zha, and H. Wang. Unlearn dataset bias in natural language inference by fitting the residual. *EMNLP-IJCNLP 2019*, page 132, 2019.
- [16] D. Hendrycks, K. Lee, and M. Mazeika. Using pre-training can improve model robustness and uncertainty. In *International Conference on Machine Learning*, pages 2712–2721. PMLR, 2019.
- [17] G. E. Hinton. Training products of experts by minimizing contrastive divergence. *Neural computation*, 14(8):1771–1800, 2002.
- [18] W. Hu, G. Niu, I. Sato, and M. Sugiyama. Does distributionally robust supervised learning give robust classifiers? In *International Conference on Machine Learning*, pages 2029–2037. PMLR, 2018.
- [19] W. Jin, R. Barzilay, and T. Jaakkola. Enforcing predictive invariance across structured biomedical domains, 2020.
- [20] Y. Kim. Convolutional neural networks for sentence classification. In *Proceedings of the 2014 Conference on Empirical Methods in Natural Language Processing (EMNLP)*, pages 1746–1751, Doha, Qatar, Oct. 2014. Association for Computational Linguistics. doi: 10.3115/v1/D14-1181. URL <https://www.aclweb.org/anthology/D14-1181>.
- [21] D. P. Kingma and J. Ba. Adam: A method for stochastic optimization. *arXiv preprint arXiv:1412.6980*, 2014.
- [22] D. Krueger, E. Caballero, J.-H. Jacobsen, A. Zhang, J. Binas, D. Zhang, R. L. Priol, and A. Courville. Out-of-distribution generalization via risk extrapolation (rex), 2020.
- [23] Y. LeCun, L. Bottou, Y. Bengio, and P. Haffner. Gradient-based learning applied to document recognition. *Proceedings of the IEEE*, 86(11):2278–2324, 1998.
- [24] T. Lei, R. Barzilay, and T. Jaakkola. Rationalizing neural predictions. In *Proceedings of the 2016 Conference on Empirical Methods in Natural Language Processing*, pages 107–117, 2016.
- [25] Z. Liu, P. Luo, X. Wang, and X. Tang. Deep learning face attributes in the wild. In *Proceedings of International Conference on Computer Vision (ICCV)*, December 2015.
- [26] R. K. Mahabadi, Y. Belinkov, and J. Henderson. End-to-end bias mitigation by modelling biases in corpora. *ACL*, 2020.
- [27] J. McAuley, J. Leskovec, and D. Jurafsky. Learning attitudes and attributes from multi-aspect reviews. In *2012 IEEE 12th International Conference on Data Mining*, pages 1020–1025. IEEE, 2012.
- [28] T. McCoy, E. Pavlick, and T. Linzen. Right for the wrong reasons: Diagnosing syntactic heuristics in natural language inference. In *Proceedings of the 57th Annual Meeting of the Association for Computational Linguistics*, pages 3428–3448, Florence, Italy, July 2019. Association for Computational Linguistics. doi: 10.18653/v1/P19-1334. URL <https://www.aclweb.org/anthology/P19-1334>.
- [29] T. Mikolov, E. Grave, P. Bojanowski, C. Puhresch, and A. Joulin. Advances in pre-training distributed word representations. In *Proceedings of the International Conference on Language Resources and Evaluation (LREC 2018)*, 2018.

- [30] Y. Oren, S. Sagawa, T. Hashimoto, and P. Liang. Distributionally robust language modeling. In *Proceedings of the 2019 Conference on Empirical Methods in Natural Language Processing and the 9th International Joint Conference on Natural Language Processing (EMNLP-IJCNLP)*, pages 4218–4228, 2019.
- [31] J. Peters, P. Bühlmann, and N. Meinshausen. Causal inference by using invariant prediction: identification and confidence intervals. *Journal of the Royal Statistical Society. Series B (Statistical Methodology)*, pages 947–1012, 2016.
- [32] S. Sagawa, P. W. Koh, T. B. Hashimoto, and P. Liang. Distributionally robust neural networks for group shifts: On the importance of regularization for worst-case generalization. *arXiv preprint arXiv:1911.08731*, 2019.
- [33] S. Sagawa\*, P. W. Koh\*, T. B. Hashimoto, and P. Liang. Distributionally robust neural networks. In *International Conference on Learning Representations*, 2020. URL <https://openreview.net/forum?id=ryxGuJrFvS>.
- [34] S. Sagawa, A. Raghunathan, P. W. Koh, and P. Liang. An investigation of why overparameterization exacerbates spurious correlations. In *International Conference on Machine Learning (ICML)*, 2020.
- [35] K. Sakaguchi, R. Le Bras, C. Bhagavatula, and Y. Choi. Winogrande: An adversarial winograd schema challenge at scale. In *Proceedings of the AAAI Conference on Artificial Intelligence*, volume 34, pages 8732–8740, 2020.
- [36] V. Sanh, T. Wolf, Y. Belinkov, and A. M. Rush. Learning from others’ mistakes: Avoiding dataset biases without modeling them. In *International Conference on Learning Representations*, 2021. URL <https://openreview.net/forum?id=Hf3qXoiNkR>.
- [37] T. Schuster, D. Shah, Y. J. S. Yeo, D. Roberto Filizzola Ortiz, E. Santus, and R. Barzilay. Towards debiasing fact verification models. In *Proceedings of the 2019 Conference on Empirical Methods in Natural Language Processing and the 9th International Joint Conference on Natural Language Processing (EMNLP-IJCNLP)*, pages 3410–3416, Hong Kong, China, Nov. 2019. Association for Computational Linguistics. doi: 10.18653/v1/D19-1341. URL <https://www.aclweb.org/anthology/D19-1341>.
- [38] A. Shafahi, P. Saadatpanah, C. Zhu, A. Ghiasi, C. Studer, D. Jacobs, and T. Goldstein. Adversarially robust transfer learning. In *International Conference on Learning Representations*, 2020. URL <https://openreview.net/forum?id=ryebG04YvB>.
- [39] J. Stacey, P. Minervini, H. Dubossarsky, S. Riedel, and T. Rocktäschel. Avoiding the Hypothesis-Only Bias in Natural Language Inference via Ensemble Adversarial Training. In *Proceedings of the 2020 Conference on Empirical Methods in Natural Language Processing (EMNLP)*, pages 8281–8291, Online, Nov. 2020. Association for Computational Linguistics. doi: 10.18653/v1/2020.emnlp-main.665. URL <https://www.aclweb.org/anthology/2020.emnlp-main.665>.
- [40] P. A. Utama, N. S. Moosavi, and I. Gurevych. Towards debiasing nlu models from unknown biases. In *Proceedings of the 2020 Conference on Empirical Methods in Natural Language Processing (EMNLP)*, pages 7597–7610, 2020.
- [41] P. Welinder, S. Branson, T. Mita, C. Wah, F. Schroff, S. Belongie, and P. Perona. Caltech-UCSD Birds 200. Technical Report CNS-TR-2010-001, California Institute of Technology, 2010.
- [42] J. Woodward. *Making things happen: A theory of causal explanation*. Oxford university press, 2005.
- [43] K. Yang, K. Swanson, W. Jin, C. Coley, P. Eiden, H. Gao, A. Guzman-Perez, T. Hopper, B. Kelley, M. Mathea, et al. Analyzing learned molecular representations for property prediction. *Journal of chemical information and modeling*, 59(8):3370–3388, 2019.

- [44] R. Zellers, A. Holtzman, Y. Bisk, A. Farhadi, and Y. Choi. HellaSwag: Can a machine really finish your sentence? In *Proceedings of the 57th Annual Meeting of the Association for Computational Linguistics*, pages 4791–4800, Florence, Italy, July 2019. Association for Computational Linguistics. doi: 10.18653/v1/P19-1472. URL <https://www.aclweb.org/anthology/P19-1472>.

## A Theoretical analysis

### A.1 Partitions reveal the unstable correlation

We start by reviewing the results in [5] which shows that the generated partitions reveal the unstable correlation. We consider binary classification tasks where  $\mathcal{Y} \in \{0, 1\}$ . For a given input  $x$ , we use  $\mathcal{C}(x)$  to represent its stable (causal) feature and  $\mathcal{Z}(x)$  to represent its unstable feature. In order to ease the notation, if no confusion arises, we omit the dependency on  $x$ . We use lowercase letters  $c, z, y$  to denote the specific values of  $\mathcal{C}, \mathcal{Z}, \mathcal{Y}$ .

**Proposition 1.** *For a pair of environments  $E_i$  and  $E_j$ , assuming that the classifier  $f_i$  is able to learn the true conditional  $P_i(\mathcal{Y} \mid \mathcal{C}, \mathcal{Z})$ , we can write the joint distribution  $P_j$  of  $E_j$  as the mixture of  $P_j^{i\checkmark}$  and  $P_j^{i\times}$ :*

$$P_j(c, z, y) = \alpha_j^i P_j^{i\checkmark}(c, z, y) + (1 - \alpha_j^i) P_j^{i\times}(c, z, y),$$

where  $\alpha_j^i = \sum_{c, z, y} P_j(c, z, y) \cdot P_i(y \mid c, z)$  and

$$P_j^{i\checkmark}(c, z, y) \propto P_j(c, z, y) \cdot P_i(y \mid c, z),$$

$$P_j^{i\times}(c, z, y) \propto P_j(c, z, y) \cdot P_i(1 - y \mid c, z).$$

*Proof.* See [5]. □

Proposition 1 tells us that if  $f_i$  is powerful enough to capture the true conditional in  $E_i$ , partitioning the environment  $E_j$  is equivalent to scaling its joint distribution based on the conditional on  $E_i$ .

Now suppose that the marginal distribution of  $\mathcal{Y}$  is uniform in all joint distributions, i.e.,  $f_i$  performs equally well on different labels. Bao et al. [5] shows that the unstable correlations will have different signs in the subset of correct predictions and in the subset of incorrect predictions.

**Proposition 2.** *Suppose  $\mathcal{Z}$  is independent of  $\mathcal{C}$  given  $\mathcal{Y}$ . For any environment pair  $E_i$  and  $E_j$ , if  $\sum_y P_i(z \mid y) = \sum_y P_j(z \mid y)$  for any  $z$ , then  $\text{Cov}(\mathcal{Z}, \mathcal{Y}; P_i) > \text{Cov}(\mathcal{Z}, \mathcal{Y}; P_j)$  implies*

$$\text{Cov}(\mathcal{Z}, \mathcal{Y}; P_j^{i\times}) < 0, \quad \text{and} \quad \text{Cov}(\mathcal{Z}, \mathcal{Y}; P_j^{i\checkmark}) > 0.$$

*Proof.* See [5]. □

Proposition 2 implies that no matter whether the spurious correlation is positive or negative, by interpolating  $P_j^{i\checkmark}, P_j^{i\times}, P_i^{j\checkmark}, P_i^{j\times}$ , we can obtain an *oracle* distribution where the spurious correlation between  $\mathcal{Z}$  and  $\mathcal{Y}$  vanishes. Since the oracle interpolation coefficients are not available in practice, Bao et al. [5] propose to optimize the worst-case risk across all interpolations of the partitions.

### A.2 Partitions reveal the unstable feature

Proposition 2 shows that the partitions  $E_j^{i\checkmark}, E_j^{i\times}, E_i^{j\checkmark}, E_i^{j\times}$  are informative of the biases. However these partitions are not transferable as they are coupled with task-specific information, i.e., the label  $\mathcal{Y}$ . To untangle this dependency, we look at different label values and obtain the following result.

**Corollary 1.** *Under the same assumption as Proposition 2, if  $\text{Cov}(\mathcal{Z}, \mathcal{Y}; P_i) > \text{Cov}(\mathcal{Z}, \mathcal{Y}; P_j) > 0$  and  $\mathcal{Z}$  follows a uniform distribution within each partition, then*

$$\begin{aligned} \sum_z z P_j^{i\times}(\mathcal{Z} = z, \mathcal{Y} = 1) &> \sum_z z P_j^{i\checkmark}(\mathcal{Z} = z, \mathcal{Y} = 1), \\ \sum_z z P_j^{i\times}(\mathcal{Z} = z, \mathcal{Y} = 0) &< \sum_z z P_j^{i\checkmark}(\mathcal{Z} = z, \mathcal{Y} = 0). \end{aligned}$$

*Proof.* By definition of the covariance, we have

$$\text{Cov}(\mathcal{Z}, \mathcal{Y}) = \sum_{z, y} zy P(\mathcal{Z} = z, \mathcal{Y} = y) - \left( \sum_z z P(\mathcal{Z} = z) \right) \left( \sum_y y P(\mathcal{Y} = y) \right)$$

Since we assume the marginal distribution of the label is uniform, we have  $\sum_y yP(\mathcal{Y} = y) = 0.5$ . Then we have

$$\text{Cov}(\mathcal{Z}, \mathcal{Y}) = \sum_z zP(\mathcal{Z} = z, \mathcal{Y} = 1) - 0.5 \sum_z zP(\mathcal{Z} = z).$$

Using  $P(\mathcal{Z} = z) = P(\mathcal{Z} = z, \mathcal{Y} = 0) + P(\mathcal{Z} = z, \mathcal{Y} = 1)$ , we obtain

$$\text{Cov}(\mathcal{Z}, \mathcal{Y}) = 0.5 \sum_z zP(\mathcal{Z} = z, \mathcal{Y} = 1) - 0.5 \sum_z zP(\mathcal{Z} = z, \mathcal{Y} = 0). \quad (2)$$

From Proposition 2, we have  $\text{Cov}(\mathcal{Z}, \mathcal{Y}; P_j^{i \times}) < 0$ . Note that this implies  $\text{Cov}(\mathcal{Z}, \mathcal{Y}; P_j^{i \vee}) > 0$  since  $\text{Cov}(\mathcal{Z}, \mathcal{Y}; P_j) > 0$  and  $P_j = \alpha_j^i P_j^{i \vee} + (1 - \alpha_j^i) P_j^{i \times}$ . Combining with Eq (2), we have

$$\begin{aligned} \sum_z zP_j^{i \times}(\mathcal{Z} = z, \mathcal{Y} = 1) &< \sum_z zP_j^{i \times}(\mathcal{Z} = z, \mathcal{Y} = 0), \\ \sum_z zP_j^{i \vee}(\mathcal{Z} = z, \mathcal{Y} = 1) &> \sum_z zP_j^{i \vee}(\mathcal{Z} = z, \mathcal{Y} = 0). \end{aligned} \quad (3)$$

Since we assume the marginal distribution of the unstable feature  $\mathcal{Z}$  is uniform, we have

$$\begin{aligned} \sum_z zP_j^{i \times}(\mathcal{Z} = z, \mathcal{Y} = 1) + \sum_z zP_j^{i \times}(\mathcal{Z} = z, \mathcal{Y} = 0) &= \sum_z zP_j^{i \times}(\mathcal{Z} = z) = 0.5, \\ \sum_z zP_j^{i \vee}(\mathcal{Z} = z, \mathcal{Y} = 1) + \sum_z zP_j^{i \vee}(\mathcal{Z} = z, \mathcal{Y} = 0) &= \sum_z zP_j^{i \vee}(\mathcal{Z} = z) = 0.5. \end{aligned} \quad (4)$$

Plugging Eq (4) into Eq (3), we have

$$\begin{aligned} \sum_z zP_j^{i \times}(\mathcal{Z} = z, \mathcal{Y} = 1) &< 0.25 < \sum_z zP_j^{i \times}(\mathcal{Z} = z, \mathcal{Y} = 0), \\ \sum_z zP_j^{i \vee}(\mathcal{Z} = z, \mathcal{Y} = 1) &> 0.25 > \sum_z zP_j^{i \vee}(\mathcal{Z} = z, \mathcal{Y} = 0). \end{aligned}$$

Combining the two inequalities finishes the proof.  $\square$

Corollary 1 shows that if we look at examples within the same label value, then expectation of the unstable feature  $\mathcal{Z}$  within the set of correct predictions will diverge from the one within the set of incorrect predictions. In order to learn a metric space that corresponds to the values of  $\mathcal{Z}$ , we sample different batches from the partitions and prove the following theorem.

**Theorem 1.** (Full version) Suppose  $\mathcal{Z}$  is independent of  $\mathcal{C}$  given  $\mathcal{Y}$ . We assume that  $\mathcal{Y}$  and  $\mathcal{Z}$  both follow a uniform distribution within each partition.

Consider examples in  $E_j$  with label value  $y$ . Let  $X_1^\vee, X_2^\vee$  denote two batches of examples that  $f_i$  predicted correctly, and let  $X_3^\times$  denote a batch of incorrect predictions. If  $\text{Cov}(\mathcal{Z}, \mathcal{Y}; P_i) > \text{Cov}(\mathcal{Z}, \mathcal{Y}; P_j) > 0$ , we have

$$\|\overline{\mathcal{Z}}(X_1^\vee) - \overline{\mathcal{Z}}(X_2^\vee)\|_2 < \|\overline{\mathcal{Z}}(X_1^\vee) - \overline{\mathcal{Z}}(X_3^\times)\|_2$$

almost surely for large enough batch size.

*Proof.* Without loss of generality, we consider  $y = 0$ . Let  $n$  denote the batch size of  $X_1^\vee, X_2^\vee$  and  $X_3^\times$ . By the law of large numbers, we have

$$\overline{\mathcal{Z}}(X_1^\vee), \overline{\mathcal{Z}}(X_2^\vee) \xrightarrow{\text{a.s.}} \mathbb{E}_{P_j^{i \vee}(\mathcal{Z}|\mathcal{Y})}[\mathcal{Z} | \mathcal{Y} = 0] \quad \text{and} \quad \overline{\mathcal{Z}}(X_3^\times) \xrightarrow{\text{a.s.}} \mathbb{E}_{P_j^{i \times}(\mathcal{Z}|\mathcal{Y})}[\mathcal{Z} | \mathcal{Y} = 0],$$

as  $n \rightarrow \infty$ . Note that Corollary 1 tells us

$$\mathbb{E}_{P_j^{i \times}(\mathcal{Z}|\mathcal{Y})}[\mathcal{Z} | \mathcal{Y} = 0] < \mathbb{E}_{P_j^{i \vee}(\mathcal{Z}|\mathcal{Y})}[\mathcal{Z} | \mathcal{Y} = 0].$$

Thus we have

$$\|\overline{\mathcal{Z}}(X_1^\vee) - \overline{\mathcal{Z}}(X_2^\vee)\|_2 < \|\overline{\mathcal{Z}}(X_1^\vee) - \overline{\mathcal{Z}}(X_3^\times)\|_2$$

almost surely as  $n \rightarrow \infty$ .  $\square$

We note that while we focus our theoretical analysis on binary tasks, empirically, our method is able to correctly identify the hidden bias for multi-dimensional unstable features and multi-dimensional label values.

## B Experimental setup

### B.1 Datasets and models

#### B.1.1 MNIST

**Data** We use the official train-test split of MNIST. Training environments are constructed from training split, with 7370 examples per environment for EVEN and 7625 examples per environment for ODD. Validation data and testing data is constructed based on the testing split. For EVEN, both validation data and testing data have 1230 examples. For ODD, the number is 1267. Following Arjovsky et al. [2], We convert each grey scale image into a  $5 \times 28 \times 28$  tensor, where the first dimension corresponds to the spurious color feature.

**Representation backbone** We follow the architecture from PyTorch’s MNIST example<sup>3</sup>. Specifically, each input image is passed to a CNN with 2 convolution layers followed by 2 fully connected layers.

**License** The dataset is freely available at <http://yann.lecun.com/exdb/mnist/>.

#### B.1.2 Beer Review

**Data** We use the script created by Bao et al. [5] to generate spurious features for each aspect. Specifically, for each aspect, we randomly sample training/validation/testing data from the dataset. Since our focus in this paper is to measure whether the algorithm is able to remove biases (rather than label imbalance), we maintain the marginal distribution of the label to be uniform. Each training environment contains 4998 examples. The validation data contains 4998 examples and the testing data contains 5000 examples. The vocabulary sizes for the three aspects (look, aroma, palate) are: 10218, 10154 and 10086.

**Representation backbone** We use a 1D CNN [20], with filter size 3, 4, 5, to obtain the feature representation. Specifically, each input is first encoded by pre-trained FastText embeddings [29]. Then it is passed into a convolution layer followed by max pooling and ReLU activation.

**License** This dataset was originally downloaded from <https://snap.stanford.edu/data/web-BeerAdvocate.html>. As per request from BeerAdvocate the data is no longer publicly available.

#### B.1.3 ASK2ME

**Data** We randomly split the data and use 50% for PENETRANCE and 50% for INCIDENCE. For PENETRANCE, there are 948 examples in  $E_1^{\text{train}}$  and  $E_1^{\text{val}}$ , 816 examples in  $E_2^{\text{train}}$  and 268 examples in  $E^{\text{test}}$ . For INCIDENCE, there are 879 examples in  $E_1^{\text{train}}$  and  $E_1^{\text{val}}$ , 773 examples in  $E_2^{\text{train}}$  and 548 examples in  $E^{\text{test}}$ . The processed data will be publicly available.

**Model** The model architecture is the same as the one for Beer review.

**License** MIT License.

#### B.1.4 Waterbird

**Data** Following Liu et al. [25], we group different classes of birds together to form binary classification tasks.

In WATERFOWL, the task is to identify 9 different waterfowls (Red breasted Merganser, Pigeon Guillemot, Horned Grebe, Eared Grebe, Mallard, Western Grebe, Gadwall, Hooded Merganser, Pied billed Grebe) against 9 different landbirds (Mourning Warbler, Whip poor Will, Brewer Blackbird, Tennessee Warbler, Winter Wren, Loggerhead Shrike, Blue winged Warbler, White crowned Sparrow, Yellow bellied Flycatcher). The training environment  $E_1^{\text{train}}$  contains 298 examples and the training

<sup>3</sup><https://github.com/pytorch/examples/blob/master/mnist/main.py>

environment  $E_2^{\text{train}}$  contains 250 examples. The validation set has 300 examples and the test set has 216 examples.

In SEABIRD, the task is to identify *36 different seabirds* (Heermann Gull, Red legged Kittiwake, Rhinoceros Auklet, White Pelican, Parakeet Auklet, Western Gull, Slaty backed Gull, Frigatebird, Western Meadowlark, Long tailed Jaeger, Red faced Cormorant, Pelagic Cormorant, Brandt Cormorant, Black footed Albatross, Western Wood Pewee, Forsters Tern, Glaucous winged Gull, Pomarine Jaeger, Sooty Albatross, Artic Tern, California Gull, Horned Puffin, Crested Auklet, Elegant Tern, Common Tern, Least Auklet, Northern Fulmar, Ring billed Gull, Ivory Gull, Laysan Albatross, Least Tern, Black Tern, Caspian Tern, Brown Pelican, Herring Gull, Eastern Towhee) against *36 different landbirds* (Prairie Warbler, Ringed Kingfisher, Warbling Vireo, American Goldfinch, Black and white Warbler, Marsh Wren, Acadian Flycatcher, Philadelphia Vireo, Henslow Sparrow, Scissor tailed Flycatcher, Evening Grosbeak, Green Violetear, Indigo Bunting, Gray Catbird, House Sparrow, Black capped Vireo, Yellow Warbler, Common Raven, Pine Warbler, Vesper Sparrow, Pileated Woodpecker, Bohemian Waxwing, Bronzed Cowbird, American Three toed Woodpecker, Northern Waterthrush, White breasted Kingfisher, Olive sided Flycatcher, Song Sparrow, Le Conte Sparrow, Geococcyx, Blue Grosbeak, Red cockaded Woodpecker, Green tailed Towhee, Sayornis, Field Sparrow, Worm eating Warbler). The training environment  $E_1^{\text{train}}$  contains 1176 examples and the training environment  $E_2^{\text{train}}$  contains 998 examples. The validation set has 1179 examples and the test set has 844 examples.

**Model** We use the Pytorch torchvision implementation of the ResNet50 model, starting from pretrained weights. We re-initialize the final layer to predict the label.

**License** This dataset is publicly available at [https://nlp.stanford.edu/data/dro/waterbird\\_complete95\\_forest2water2.tar.gz](https://nlp.stanford.edu/data/dro/waterbird_complete95_forest2water2.tar.gz)

## B.2 Implementation details

**For all methods:** We use batch size 50 and evaluate the validation performance every 100 batch. We apply early stopping once the validation performance hasn’t improved in the past 20 evaluations. We use Adam [21] to optimize the parameters and tune the learning rate  $\in \{10^{-3}, 10^{-4}\}$ . For simplicity, we train all methods without data augmentation. Following Sagawa et al. [32], we apply strong regularizations to avoid over-fitting. Specifically, we tune the dropout rate  $\in \{0.1, 0.3, 0.5\}$  for text classification datasets (Beer review and ASK2ME) and tune the weight decay parameters  $\in \{10^{-1}, 10^{-2}, 10^{-3}\}$  for image datasets (MNIST and Waterbird).

**Ours** We fix  $\delta = 0.3$  in all our experiments. Based on our preliminary experiments (Figure 5), we fix the number of clusters to be 2 for all our experiments in Table 2. For the target classifier, we directly optimize the min – max objective. Specifically, at each step, we sample a batch of example from each group, and minimize the worst-group loss. We found the training process to be pretty stable when using the Adam optimizer.

**Validation criteria** For ERM, REUSE, FINETUNE and MULTITASK, since we don’t have any additional information (such as environments) for the target data, we apply early stopping and hyper-parameter selection based on the average accuracy on the validation data.

For TOFU, since we have already learned an unstable feature representation  $f_Z$  on the source task, we can also use it to cluster the validation data into groups where the unstable features within each group are different. We measure the worst-group accuracy and use it as our validation criteria.

For ORACLE, as we assume access to the oracle unstable features for the target data, we can use them to define groups on the validation data as well. We use the worst-group accuracy as our validation criteria.

We also note that when we transfer from LOOK to AROMA in Table 2, both TOFU and ORACLE are able to achieve 75 accuracy on  $E^{\text{test}}$ . This number is higher than the performance of training on AROMA with two data environments ( 68 accuracy in Table 2). This result makes sense since in the latter case, we only have in-domain validation set and we use the average accuracy as our hyper-parameter selection metric. However, in both TOFU and ORACLE, we create (either automatically or manually) groups over the validation data and measure the worst-group performance. This ensures that the chosen model will not over-fit to the unstable correlations.

Table 4: Illustration of the tasks on MNIST for multiple source tasks experiments. In the source tasks ( $S_1, S_2, S_3$ ), we want to classify two digits where the label is spuriously correlated with a color pair (red-blue, red-green, blue-green). In the target task  $T$ , the goal is to learn a color-invariant model by using only one *biased* environment  $E_1^{\text{train}}$ .

Tasks	Labels	$E_1^{\text{train}}$	$E_2^{\text{train}}$	$E^{\text{test}}$
$S_1$	0 vs. 1	0000000000 1111111111	0000000000 1111111111	0000000000 1111111111
$S_2$	2 vs. 3	2222222222 3333333333	2222222222 3333333333	2222222222 3333333333
$S_3$	4 vs. 5	4444444444 5555555555	4444444444 5555555555	4444444444 5555555555
$T$	6 vs. 7 vs. 8	6666666666 7777777777 8888888888	NA	6666666666 7777777777 8888888888

**Computational resources:** We use our internal clusters (24 NVIDIA RTX A6000 and 16 Tesla V100-PCIE-32GB) for the experiments. It took around 3 days to generate all the results in Table 2.

## C Multiple source tasks

One major limitation of our work is that the source task and the target task need to share the same unstable features. While a single source task may not describe all unwanted unstable features, we can leverage multiple source tasks and combine their individual unstable features together.

**Extending TOFU to multiple source tasks** We can naturally extend our algorithm by inferring a *joint* unstable feature space across all source tasks.

- MS.1** For each source task  $S$  and for each source environment  $^S E_i$ , train an environment-specific classifier  $^S f_i$ .
- MS.2** For each source task  $S$  and for each pair of environments  $^S E_i$  and  $^S E_j$ , use classifier  $^S f_i$  to partition  $^S E_j$  into two sets:  $^S E_j^{\text{✓}}$  and  $^S E_j^{\text{✗}}$ , where  $^S E_j^{\text{✓}}$  contains examples that  $^S f_i$  predicted correctly and  $^S E_j^{\text{✗}}$  contains those predicted incorrectly.
- MS.3** Learn an unstable feature representation  $f_Z$  by minimizing Eq (1) across all source tasks  $S$ , all pairs of environments  $^S E_i, ^S E_j$  and all possible label value  $y$ :

$$f_Z = \arg \min \sum_S \sum_{y, ^S E_i \neq ^S E_j} \mathbb{E}_{X_1^{\text{✓}}, X_2^{\text{✓}}, X_3^{\text{✗}}} [\mathcal{L}_Z(X_1^{\text{✓}}, X_2^{\text{✓}}, X_3^{\text{✗}})],$$

where batches  $X_1^{\text{✓}}, X_2^{\text{✓}}$  are sampled uniformly from  $^S E_j^{\text{✓}}|_y$  and batch  $X_3^{\text{✗}}$  is sampled uniformly from  $^S E_j^{\text{✗}}|_y$  ( $\cdot|_y$  denotes the subset of  $\cdot$  with label value  $y$ ).

On the target task, we use this joint unstable feature representation  $f_Z$  to generate clusters as in Section 3.2. Since  $f_Z$  is trained across the source tasks, the generated clusters are informative of all unstable features that are present in these tasks. By minimizing the worst-case risks across the clusters, we obtain the final stable classifier.

**Experiment setup** We design controlled experiments on MNIST to study the effect of having multiple source tasks. We consider three source tasks:  $S_1$  (0 vs. 1),  $S_2$  (2 vs 3) and  $S_3$  (4 vs. 5). For the target task  $T$ , the goal is to identify 6, 7 and 8.

Similar to Section 4, we first generated the observed noisy label based on the digits. We then inject spurious color features to the input images. For  $S_1, S_2$  and  $S_3$ , the noisy labels are correlated with red/blue, red/green and blue/green respectively. For the target task  $T$ , the three noisy labels (6/7/8) are correlated with all three colors red/blue/green. Table 4 illustrate the different spurious correlations across the tasks.

Table 5: Target task testing accuracy of different methods on MNIST with different combinations of the source tasks (see Table 4 for an illustration of the tasks). Majority baseline is 33%. All methods are tuned based on a held-out validation set that follows from the same distribution as the target training data. Bottom right: standard deviation across 5 runs. Upper right: avg. source task testing performance (if applicable).

SOURCE	ERM	REUSE	FINETUNE	MULTITASK	TOFU	ORACLE
$S_1$	$26.8 \pm 2.4$	$34.7^{(72.0)}_{\pm 5.0}$	$35.1^{(71.9)}_{\pm 2.4}$	$17.7^{(69.4)}_{\pm 0.3}$	<b><math>57.3 \pm 6.9</math></b>	$72.7 \pm 0.7$
$S_2$	$26.8 \pm 2.4$	$34.6^{(68.0)}_{\pm 1.7}$	$31.0^{(66.7)}_{\pm 0.8}$	$14.6^{(74.5)}_{\pm 2.3}$	<b><math>57.8 \pm 8.3</math></b>	$72.7 \pm 0.7$
$S_3$	$26.8 \pm 2.4$	$34.1^{(70.2)}_{\pm 0.8}$	$33.6^{(66.3)}_{\pm 0.7}$	$12.9^{(71.2)}_{\pm 3.4}$	<b><math>49.8 \pm 5.2</math></b>	$72.7 \pm 0.7$
$S_1 + S_2$	$26.8 \pm 2.4$	$34.0^{(67.9)}_{\pm 13.9}$	$18.3^{(68.2)}_{\pm 3.2}$	$22.2^{(71.3)}_{\pm 3.0}$	<b><math>52.9 \pm 1.0</math></b>	$72.7 \pm 0.7$
$S_1 + S_3$	$26.8 \pm 2.4$	$49.9^{(70.3)}_{\pm 15.7}$	$48.3^{(68.7)}_{\pm 15.3}$	$20.3^{(72.3)}_{\pm 2.8}$	<b><math>53.4 \pm 2.3</math></b>	$72.7 \pm 0.7$
$S_2 + S_3$	$26.8 \pm 2.4$	$49.5^{(71.3)}_{\pm 7.5}$	$50.9^{(72.0)}_{\pm 12.0}$	$18.5^{(74.6)}_{\pm 7.5}$	<b><math>53.4 \pm 4.1</math></b>	$72.7 \pm 0.7$
$S_1 + S_2 + S_3$	$26.8 \pm 2.4$	$34.1^{(69.0)}_{\pm 16.4}$	$40.3^{(68.5)}_{\pm 26.3}$	$26.4^{(71.0)}_{\pm 1.2}$	<b><math>72.3 \pm 1.5</math></b>	$72.7 \pm 0.7$

**Baselines** Since ERM and ORACLE only depend on the target task, they are the same as we described in Section 4. For REUSE and FINETUNE, we first use multitask learning to learn a shared feature representation across all tasks. Specifically, for each source task, we first partition its data into subsets with opposite spurious correlations by contrasting its data environments  $E_1^{\text{train}}$  and  $E_2^{\text{train}}$  [5]. We then train a joint model, with a different classifier head for each source task, by minimizing the worst-case risk over all these subsets for each source task. The shared feature representation is directly transferred to the target task. The baseline MULTITASK is similar to REUSE and FINETUNE. The difference is that we jointly train the target task classifier together with all source tasks’ classifiers.

**Results** Table 5 presents our results on learning from multiple source tasks. Compared with the baselines, TOFU achieves the best performance across all 7 transfer settings.

We observe that having two tasks doesn’t necessarily improve the target performance for TOFU. This result is actually not surprising. For example, let’s consider having two source tasks  $S_1$  and  $S_2$ . TOFU learns to recognize red vs. blue from  $S_1$  and red vs. green from  $S_2$ , but TOFU doesn’t know that blue should be separated from green in the unstable feature space. Therefore, we shouldn’t expect to see any performance improvement when we combine  $S_1$  and  $S_2$ . However, if we have one more source task  $S_3$  which specifies the invariance between blue and green, TOFU is able to achieve the oracle performance.

For the direct transfer baselines, we see that MULTITASK simply learns to overfit the spurious correlation and performs similar to ERM. REUSE and FINETUNE generally perform better when more source tasks are available. However, their testing performance vary a lot across different runs.